JOURNAL OF CATALYSIS 100, 250–263 (1986)

Mechanism of the Deactivation of Hopcalite Catalysts Studied by XPS, ISS, and Other Techniques

S. VEPŘEK, D. L. COCKE,[1] S. KEHL, AND H. R. OSWALD

Institute of Inorganic Chemistry, University of Zürich, Winterthurerstr. 190, CH-8056 Zürich, Switzerland

Received August 28, 1985; revised December 3, 1985

A detailed study of the thermal deactivation of a commercial Hopcalite catalyst, "$CuMn_2O_4$," has been made by a multitechnique catalyst characterization approach using XPS, ISS, XRD, SEM, TA, BET, and activity testing. It is shown for the first time that the deactivation is due to segregation of the potassium component to the surface of the catalyst. The driving force of the segregation is the amorphous-to-spinel phase change at >773 K. Deactivation in N_2 or O_2 at 823 K resulted in a restructuring of the outer surface zone of the catalyst with Cu being enhanced relative to Mn. The deactivation and the concomitant phase change are accompanied by a change in the dominant oxidation state of Cu from Cu^{2+} to Cu^{1+} and of Mn from Mn^{3+} to Mn^{4+}. The oxidation state change is associated with the formation of the spinel phase where the coupled redox reaction $Cu^{2+} + Mn^{3+} \leftrightharpoons Cu^{1+} + Mn^{4+}$ is experimentally supported in the XPS data by the chemical shifts and shake-up structure (Cu), and by multiplet splitting (Mn). Plasma chemical reoxidation has been used to reestablish Cu^{2+} at the catalyst surface at a low temperature and nonequilibrium conditions. This study reveals the phenomenon of phase-change-induced segregation of a promoter when the ionic radius or the oxidation state precludes its accommodation in the lattice.

INTRODUCTION

Hopcalite, "$CuMn_2O_4$," is a well-known oxidation catalyst (*1–3*) at room temperature. This catalyst system is important in respiratory protection in military, mining, and space applications (*4–6*). It is highly active in the amorphous state but has generally been observed to lose activity at temperatures above ~773 K where crystallization of the spinel, $CuMn_2O_4$, occurs (*7–10*). However, crystalline $CuMn_2O_4$ has also been reported to be active (*11*).

The structure and oxidation states of the components of "$CuMn_2O_4$" have been difficult to determine (*12–24*). The ionization state of Cu in copper manganite is different from that of the other isomorphous compounds such as $CuFe_2O_4$ and $CuCr_2O_4$ where it is Cu^{2+}. In addition Mn is generally present as Mn^{3+} whereas in $CuMn_2O_4$ it is likely to be Mn^{4+} (*20*). It has also been reported that it is impossible to prepare stoichiometric $CuMn_2O_4$ which is cubic at room temperature (*24*) and that it can only be cubic with excess Cu ($x = 0.05$) for $Cu_{1+x}Mn_{2-x}O_4$. The nature of any surface phases have not been examined. The latest results on the bulk structure indicate that Cu^{1+}(tetrahedral) and Mn^{4+}(octahedral) is the most stable configuration in Cu–Mn spinels (*24*).

Little is known about the active sites in this catalyst, the role of the Cu "promoter," the mechanism of oxidation, or the mechanisms of deactivation. The catalyst is usually activated at temperatures above which water loss occurs. With water loss it has been suggested that Mn^{3+} (as MnOOH) is transformed to Mn^{4+} (*9, 10*) which should be an active site for O_2 adsorption. This speculation does not agree conceptually with either the acid–base properties of the reactants (CO and O_2) or the relative basicity of hydrated Cu and Mn oxide surfaces. A coupled dehydration reaction between hydrated Cu and Mn oxides can be envisioned. Here the acid–base properties of

[1] Visiting Professor. Permanent address: Department of Chemistry, Texas A&M University, College Station, Texas 77843.

0021-9517/86 $3.00

the reactants aid the thinking. CO is basic (*25, 26*) and O_2 is acidic (*25*) in the Lewis sense. Because of relative acid–base properties it can be expected that hydrated Cu oxide will dehydroxylate and hydrated Mn oxide will deprotonate to form water. This would generate relatively unstable Cu^{3+} (*27*), and Mn^{3+} would remain unchanged. However, the excess electron on $MnOO^-$ would be transferred to Cu^{3+} producing Cu^{2+}. In this way the following redox couples and their adsorption properties would be produced:

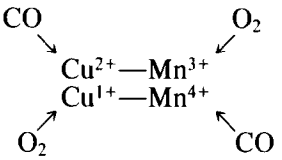

Supporting this model is the fact that both Cu_2O and MnO_2 are active CO oxidation catalysts (*3*). In addition, this is supported by the observation of Kanungo (*9, 10*) that the maximum activity occurs for Cu mole fraction of 0.5 coincidental with the maximum H_2O content and the maximum Mn^{3+}/Mn^{4+} ratio. In this context, the oxidation activity of $CuMn_2O_4$ has been attributed by Schwab and Kanungo (*11*) to Mn^{4+} where

$$CO + Mn^{4+} \rightarrow CO^+_{ads} + Mn^{3+}$$

occurs. The promotion by Cu has further been tied to the reduction of O_2

$$\tfrac{1}{2}\, O_2 + Cu^{1+} \rightarrow Cu^{2+} + O^-_{ads}$$

by these authors. The oxidation occurs by the process

$$O^-_{ads} + CO^+_{ads} \rightarrow CO_2$$

and the much discussed (*9–12, 19–21*) resonance reaction system

$$Cu^{2+} + Mn^{3+} \leftrightharpoons Cu^{1+} + Mn^{4+}$$

brings the catalyst back to the active state. If the above applies, the deactivation of this catalyst system can hardly be tied to the oxidation state of Cu or Mn as long as the redox couple remains active.

From the previous work it is not clear why the amorphous Hopcalite catalyst deactivates at the crystallization temperature. This question is the main emphasis of this paper and illustrates the requirement of a multitechnique approach in characterization of the Hopcalite catalyst system. This approach has been lacking so far.

The methods of X-ray diffraction (XRD) (*7–11*), thermal analysis (*7–12*), surface area determination (*10, 22*), and activity measurements (*7–11, 21, 23*), and the transient rate tracer technique (*28*) have been applied to study Hopcalite catalysts. Obviously missing have been applications of surface analysis techniques. Indirect measurements of surface excess oxygen by KI and hydrazine (*9, 10, 29*) have been used.

Since heterogeneous catalysis occurs on the very outer surface of solids, previous activity studies correlated with bulk composition (*9, 10*) and structural changes are in doubt. This is particularly true where commercial samples have been examined (*7, 8*).

Commercial oxidation catalysts usually have electronic (*30*) and structural promoters added (*31*) which although generally present in small amounts strongly affect activity and/or selectivity. They must also be considered in deactivation mechanisms.

In this work we use a multitechnique characterization approach with emphasis on the surface sensitive tools, X-ray photoelectron spectroscopy (XPS) and ion scattering spectroscopy (ISS), to study the deactivation of a commercial Hopcalite CO oxidation catalyst.

EXPERIMENTAL

Catalyst Data

The present study has been carried out with a Hopcalite catalyst purchased from Auergesellschaft, Berlin, F.R.G. Granule size was 1.0–1.5 mm. The catalyst was X-ray amorphous in the as-received condition and after activation according to the commercial specification. It was established

that the activity behavior of this catalyst is very similar to other commercially available catalysts or those prepared according to Refs. (*32, 33*).

The composition of the catalyst as determined by neutron activation analysis (NAA) is as follows for the minor constituents (in ppm): K 7170, Ca 4600, Fe 1850, Zn 320, Br 226, Co 158, As 70, Sb 20, Cr 9, and Ag 2.7. X-Ray emission (EDAX) analysis gave the Cu/Mn ratio 1 : 2. The activation and deactivation have been done under controlled gas flow at ~493 K in pure oxygen and 823 K in pure nitrogen (or oxygen), respectively. The deactivation also occurs at 823 K in air.

Activity Testing (Oxidation of CO)

Oxidation of CO was performed by passing a mixture of 4.97 vol% CO in air at constant flow rate (35 ml/min) through a thermostated linear reactor containing about 1 g catalyst. The measurement procedure followed that described by Schwab and Kanungo (*11*). The gas from the reactor was bubbled through a known amount of $Ba(OH)_2$ solution. The extent of conversion was calculated from the CO_2 required to neutralize a standard solution. Conversion is then proportional to the reciprocal of time and is taken as a measure of the relative activity of the catalysts.

Low-Pressure Plasma Reoxidation

In the course of this study it became necessary to establish the role of the oxidation state of copper without changing the structural and morphological properties of the deactivated catalyst. We found that Cu^{2+} is reduced to Cu^{1+} during the phase transition even in the presence of pure oxygen at 1 atm and 823 K. The loss in activity might be due to the oxidation state change of copper.

A low-pressure electrical glow discharge (*34*) of pure oxygen was used to activate the O_2 for the Cu^{1+} to Cu^{2+} conversion. Since a plasma discharge can activate oxygen under mild thermal conditions, the structural and morphological properties of the deactivated catalyst should be maintained. The discharge was excited by an 80-MHz RF generator in a silica glass tube with external sleeve electrodes. The typical conditions of treatment were: 573–623 K, pressure about 1.3 mbar, and duration of treatment of 1 to 2 h.

Methods of Characterization

Characterization of any aspect of a heterogeneous catalyst that is to be correlated to activity requires multiple techniques (*35*). Until now Hopcalite catalysts have not been properly characterized. The methods and instruments used for the catalyst characterization in this study are summarized in Table 1. The following characteristics of the Hopcalite catalyst along with the method used are as follows: bulk composition (NAA, EDAX), morphology (SEM), surface area (BET), bulk structure (XRD), thermal properties (TG/DTA), surface chemistry, structure, and composition (XPS), and surface composition and its depth profile (ISS).

In a typical surface analytical experiment, the samples were either ground and pressed into a disk and treated, or treated and mounted as particles. They were then introduced into a preparation chamber and pumped overnight at <353 K in order to decrease the outgassing. The typical background pressure in the analytical chamber was $<5 \times 10^{-10}$ and $<1 \times 10^{-8}$ mbar without and with the sample present, respectively.

RESULTS

Activity, Surface Area, and Structural Changes

Table 2 summarizes these results. They are in fair agreement with those reported by others (*7–11*). The surface area increases on activation and decreases at the amorphous-to-spinel transition. The activity increases on activation and decreases at the phase transition. Activation apparently involves water removal, thereby generating adsorption sites for O_2 and creating small

TABLE 1

Summary of the Methods and Instruments Used

Technique	Instrument	Instrumental conditions	Sample preparation
XPS	Leybold-Heraeus LHS-10	Al$K\alpha_1$, 12 kV/30 mA, $\Delta E/E$ = const. Mg$K\alpha$, 12 kV/30 mA, ΔE = const.	Ground and pressed into disks or mounted granules
ISS	LHS-10	$^4He^+$, 1 keV, rastered ion beam 2×2 mm^2	Ground and pressed into disks
XRD	Guinier IV Camera Enraf-Nonius, Holland	Fe$K\alpha_1$ (monochromatized)	Ground
TG/DTA	TA 2000-C Mettler	N_2, 1 atm ~ 40 ml/min, dT/dT = 5 K/min	As received (granules)
SEM	Cambridge Stereoscan	20 kV	Granular
EDAX	Cambridge Stereoscan	20 kV	Granular
BET	Carlo Erba Milano	N_2, 77 K	Granular

pores causing the activity to increase and the surface area to increase, respectively. Of particular interest is the lack of an unambiguous correlation between the activity and the specific area. Upon activation, both show a nominal increase of 20 to 25% but after deactivation, the activity decreases by a factor of ~20, whereas the area decreases only by a factor of $\lesssim$5. This shows that the deactivation is due largely to surface and/or structural properties of the catalyst. The decrease of the area is qualitatively seen in the scanning electron photomicrographs in Fig. 1. Considerable agglomerization and

TABLE 2

Activity, Surface Area, and Structural Changes

Treatment method	As received	Activated	Deactivated	Deactivated and plasma reoxidized
Surface area m^2/g	100	120	20–50	—
Activity % conversion	68.9	93.2	4.7	~5
Structure	Amorphous	Amorphous	$CuMn_2O_4$ [cubic]	$CuMn_2O_4$ [cubic]

Temperature vs. structure

Temperature of treatment (K)	Compound	Structure
RT	Amorphous	—
623	Amorphous	Two very weak lines corresponding to $CuMn_2O_4$ spinel
823	$CuMn_2O_4$	Cubic, spinel
1373	$CuMn_2O_4$	Cubic
	Mn_3O_4	Tetragonal (two lines)
	$CuMnO_2$	Monoclinic

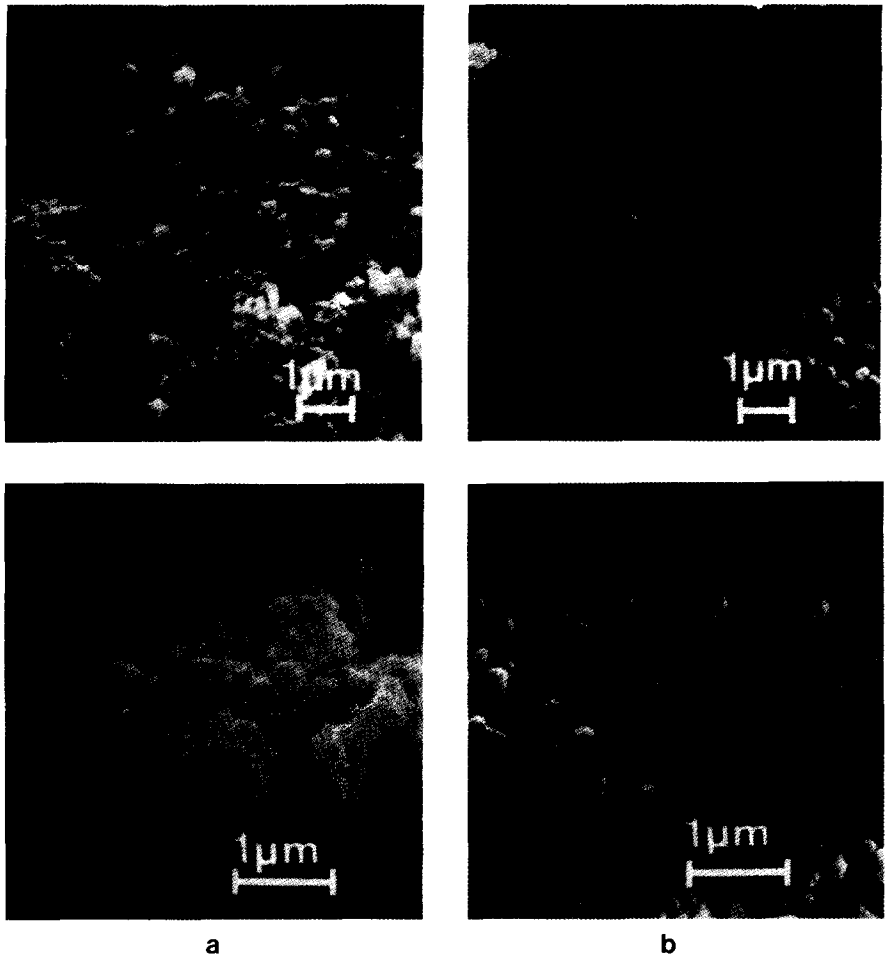

FIG. 1. Scanning electron photomicrograph of Hopcalite catalyst surfaces. (a) activated in 1 atm O_2 at 220°C for 3 h; (b) deactivated in 1 atm N_2 at 550°C for 1 h.

sintering has occurred during the amorphous-to-crystalline transition. Crystallization of amorphous catalysts is known to cause extensive sintering (*36*).

The first indication of crystalline, $CuMn_2O_4$, formation is seen by XRD at 623 K (Table 2), and the crystallization is completed at 823 K. This is in good agreement with the data on the decrease of the activity reported previously (*7–10*) and verified in the present work. Continued heating at higher temperatures causes decomposition (endotherm at 1173 K) and above 1373 K, $CuMn_2O_4$, $CuMnO_2$, and Mn_3O_4 form.

Thermal Analysis

Differential thermal analysis (DTA) and thermogravimetric analysis (TG) data are shown in Fig. 2. There are three main thermal effects. The two endothermic peaks at ~373 and 573 K are associated with the desorption of physisorbed and chemisorbed water, respectively. The exothermic peak at ~773 K is due to the crystallization of the $CuMn_2O_4$ spinel. The endothermic response at ~1173 K is due to the decomposition of the spinel. These results are in agreement with the published data (*7–10,*

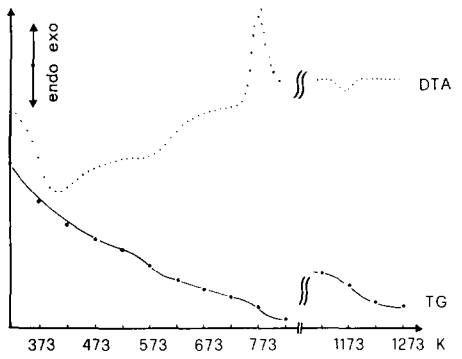

FIG. 2. Thermogravimetric and Differential Thermal Analysis of Hopcalite catalyst in a nitrogen flow of about 40 cm^3 min^{-1} at 1 atm. Heating rate 5 K/min, sample weight about 45 mg.

37). In particular, the temperature range for the phase transition agrees with the coprecipitated catalyst prepared by Dondur *et al.* (*7, 8*) whereas the commercial catalysts had a somewhat higher (~50 K) transition temperature. This indicates that structural stabilization by promoters in the catalyst under study are minimal.

Surface Studies, XPS

X-Ray photoelectron spectroscopy (XPS) is an established catalyst characterization tool. Dreiling (*38*) has shown that XPS can resolve the cuprous and cupric components of $CuMn_2O_4$ and follow the changes in these with thermal treatments. However, XPS has not been previously used to study the catalytically important parameters of Hopcalite catalysts. XPS has been used in this study to examine changes in surface and subsurface composition and the oxidation state of the copper and manganese as they are affected by thermal treatments in various environments (i.e., activation and deactivation).

Survey spectra (1000 eV) of activated, deactivated and plasma reoxidized samples are shown in Fig. 3. The obvious differences between the spectra are seen in the Cu 2*p* region, in the Cu($L_3M_{4,5}M_{4,5}$) Auger signal and in the intensity of the K 2*p* core line. Carbon as revealed by the C 1*s* line is generally present at a low, almost constant level.

Detail of the Cu 2*p* region is shown in Fig. 4. The main features in this spectral region are the spin-orbit split $2p_{1/2}$ and $2p_{3/2}$ peaks along with their shake-up satellites. Cu^{2+} has satellite features while Cu^{1+} does not (*38, 39*). The major differences are seen in the relative intensities of the satellites at $\sim E_b$ = 963 and 944 eV and the binding energy of the core level $2p_{3/2}$ and $2p_{1/2}$ peaks. The deactivation of the catalyst is seen to be accompanied by a decrease of the intensities of the satellites and a shift of the main peaks to lower binding energy. This is caused by a decrease of the Cu^{2+} concentration in the near surface zone. Deactivation in oxygen causes a smaller effect than deactivation in nitrogen.

Upon plasma reoxidation, the shake-up satellite structure is fully recovered but the

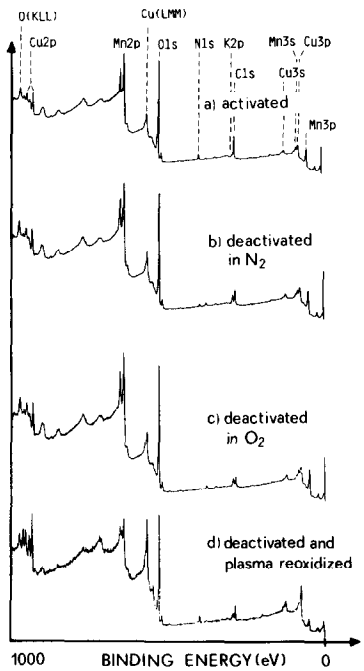

FIG. 3. XPS survey spectra of Hopcalite catalyst after various treatments. (a) Activated, 1 atm O_2 for 3 h; (b) deactivated, 1 atm N_2 for 1 h; (c) deactivated, 1 atm O_2 for 1 h; (d) deactivated in 1 atm N_2 and reoxidized in oxygen plasma, <300°C, 2 h. Al$K\alpha$ radiation, $\Delta E/E$ = const., retarding factor 10.

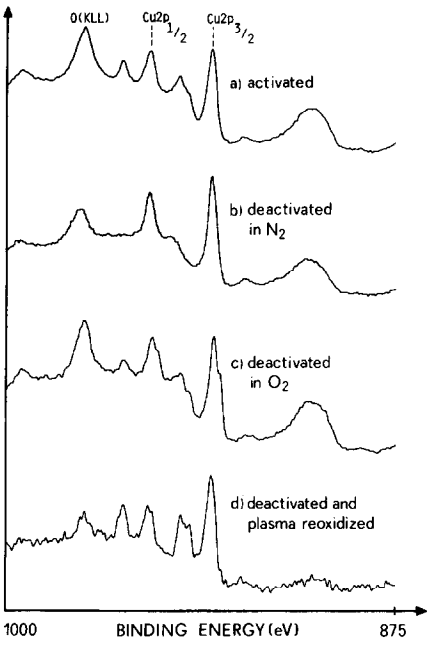

FIG. 4. Detail of the Cu 2*p* region of the survey spectra shown in Fig. 3. The binding energies of Cu $2p_{1/2}$ and Cu $2p_{3/2}$ are 954.2 and 934.5 eV for activated, and 950.2 and 930.5 eV for deactivated catalysts, respectively (see Table 3). These shifts are not quite resolved in the figure because of small charging of the samples. Therefore, the C 1*s* signal was used for exact energy calibration (see text).

catalytic activity is not noticeably increased. The increase of the intensity of the Cu($L_3M_{4,5}M_{4,5}$) Auger signal as compared to that of the deactivated and activated samples shows copper enrichment in the near surface region has occurred upon oxygen plasma treatment (Fig. 3). As shown in Fig. 5, this effect is reflected in the Cu 3*p* peak as compared to the Mn 3*p*.

A close view of the intensity changes of the K $2p_{3/2}$ line (Fig. 3) shows that surface enrichment of potassium occurs upon deactivation and it remains approximately constant after oxygen plasma treatment. On the other hand, there are no comparable changes of the intensity of the Ca $2p_{1/2,3/2}$ line ($E_b \sim 350$ eV) seen during the phase change and deactivation. Since XPS is sensitive to several atomic layers (*47*) of the catalyst, the location of the potassium at the outer surface is suggested, but not confirmed. Consequently ion scattering experiments were performed to establish the details of the location of potassium.

The binding energies for carbon, oxygen, manganese and copper are summarized in Table 3.

The binding energies for oxygen are typical for the oxide ion, O^{2-}. The binding energy for carbon is chosen at 285.0 eV and used to calibrate for small charging shifts when they occurred.

For the activated catalysts, Cu $2p_{3/2}$ binding energies are due mainly to Cu^{2+} with a binding energy of 934.5 eV. This binding energy is close to that found by d'Huysser *et al.* (*40*) for Cu^{2+} in an octahedral environment. For the deactivated catalysts, the binding energies are shifted ~4 eV to lower binding energies. This binding energy is lower than that generally observed for Cu^{1+} in Cu_2O and Cu^0 in metallic copper. However, such low binding energies for Cu^{1+} have been found for Cu^{1+} in ferrites and chromites in octahedral symmetry (*40, 41*) and in molybdates by Haber *et al.* (*42*).

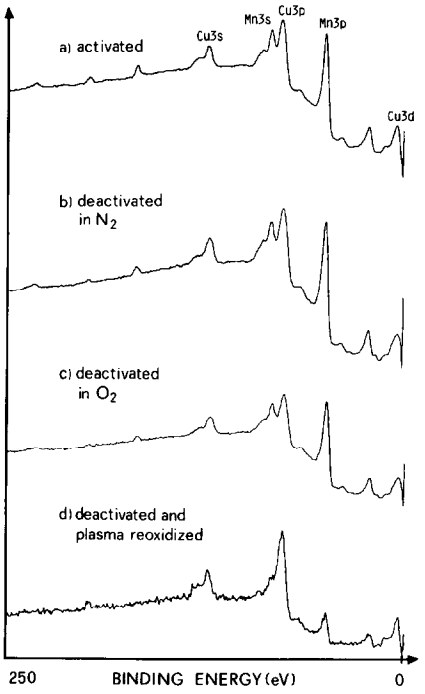

FIG. 5. Detail of the survey spectra of Fig. 3 in the low binding energy region.

TABLE 3

Binding Energies of the Principal XPS Lines in Hopcalite Corrected to E_b(C 1*s*) = 285 eV

	Activated in O_2 at 220°C	Deactivated in N_2 at 550°C	Cu metal
Cu $2p_{3/2}$	934.5	930.5	932.2
Cu $2p_{1/2}$	954.2	950.2	952.0
Mn $2p_{3/2}$	642.0	641.0	—
Mn $2p_{1/2}$	652.3	651.5	—
O 1*s*	529.0	529.0	—
K $2p_{3/2}$	—	293.0	—
K $2p_{1/2}$	—	295.5	—
Cu 3*s*	122.7	121.6	—
Cu 3*p*	76.0	75.5	—
Mn 3*s*	83.3	83.0	—
Mn 3*p*	48.6	48.5	—

Since the "chemical shift" is mainly due to the initial charge state, the Madelung potential and final state relaxation energy, these latter authors attribute the negative binding energy shift with respect to Cu^0 to the difference in the Madelung potential. It thus appears that in the deactivated catalyst, the oxide surface region is dominated by Cu^{1+} in octahedral environment.

The shifts in the Mn electron binding energies if they occur are within the instrumental resolution used. Thus the oxidation state of Mn was not determined from the chemical shifts in this work. However, the 3*s* multiplet splitting has been shown by Shirley (*44*) to decrease by about one eV per electron removed for $Mn^{2+}(3d^5)$, $Mn^{3+}(3d^4)$, and $Mn^{4+}(3d^3)$. This has been used to establish the oxidation states of Mn in the various treated Hopcalites. The multiplet splitting has been previously used to examine the oxidation states of Mn in manganese spinels (*43*). The Mn 3*s* region is shown in Fig. 6. It is seen that the activated amorphous catalyst has somewhat broader peaks as one would expect from the range of coordination found in amorphous materials. The satellite position is indicative of Mn^{3+} with some smaller contribution from Mn^{4+}. The catalyst deactivated in N_2 clearly has Mn^{4+} in a discrete symmetry. Mn^{4+} with $3d^3$ electronic configuration is probably in octrahedral symmetry as predicted (*23, 24*). The plasma reoxidized catalyst shows both Mn^{3+} and Mn^{4+} satellites. Thus the following is established:

Activated	Cu^{2+}	Mn^{3+}
Deactivated	Cu^{1+}	Mn^{4+}
Plasma reoxidized	Cu^{2+}	$Mn^{3+}(Mn^{4+})$

On those occasions when both Cu^{2+} and Cu^{1+} have been observed (i.e., deactivation in air or oxygen) both Mn^{3+} and Mn^{4+} have also been present.

Surface Studies, ISS

The application of ion scattering spectroscopy (ISS) to characterize heterogeneous catalysts has been limited. However, its use is being extended to several hetero-

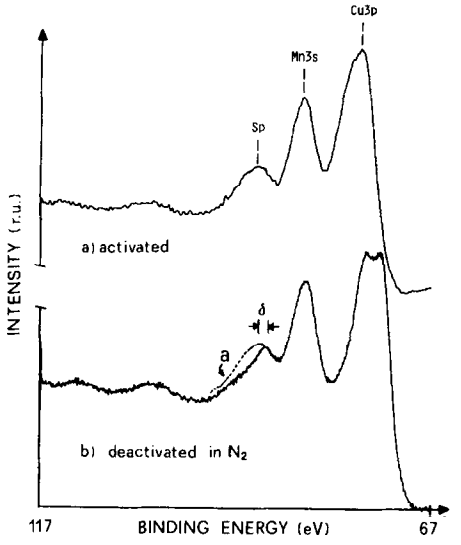

FIG. 6. Detail spectrum of the Mn 3*s* region showing the decrease of the multiplet splitting due to the decrease of the number of Mn 3*d* electrons upon deactivation ($Mn^{3+} \rightarrow Mn^{4+}$). (a) Activated; (b) deactivated. Mg$K\alpha$ radiation, ΔE = const., transmission energy 100 eV.

geneous catalytic systems such as those used in hydrodesulfization and hydrocracking. The principles of ISS and a summary of ISS catalyst characterization can be found in a recent review (*45*). It has monolayer sensitivity and can give detailed structural information by depth profiling through the outer three to four atomic layers. Beyond this, statistical mixing causes loss of information. It has, however, been able to delineate the layered structure of Co–Mo and Ni–Mo/alumina catalysts (*46*) and their thermally induced structural changes. It is used in this work for a similar purpose.

A typical sequence of ISS spectra as a function of sputtering time is shown in Fig. 7 for the activated, deactivated and plasma reoxidized catalysts. The dominance of the potassium peak in the spectra for the deactivated catalyst shows that the surface of the deactivated catalyst is completely covered by a potassium overlayer. Although ISS cannot resolve the signals from K and Ca the features observed in Fig. 7 are due to K because of the absence of any changes in the corresponding energy regions of the Ca 2*p* signal in the XPS spectrum (Fig. 3). Furthermore, because of a relatively small radius of Ca^{2+} compared to K^{1+}, no significant segregation of Ca is expected to occur upon crystallization of the catalyst, although its concentration in Hopcalite is only slightly less than that of K. At the beginning no Cu or Mn is visible, indicating

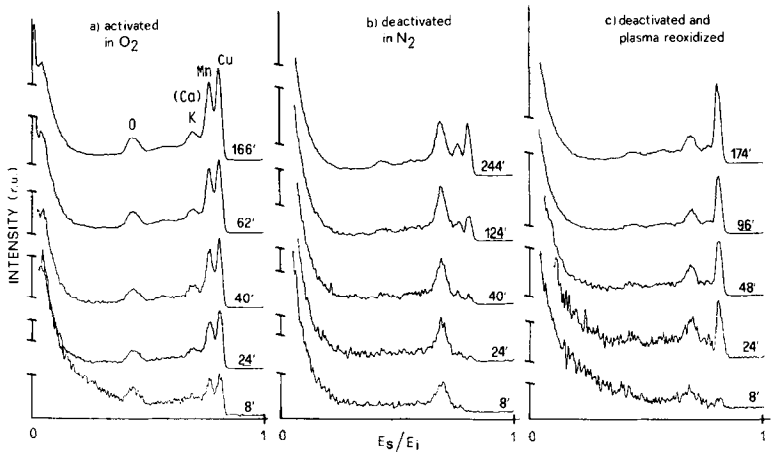

FIG. 7. Selected examples of typical sequences of the ISS spectra as a function of sputtering time. (a) Activated; (b) deactivated; (c) deactivated and plasma reoxidized (as in Fig. 3). $^4He^+$, 1 keV, $\Delta E/E$ = const., retarding factor 3. Typical sampling time: 4 to 10 min. E_s/E_i: the ratio of the scattered to the incident He^+ ion energy.

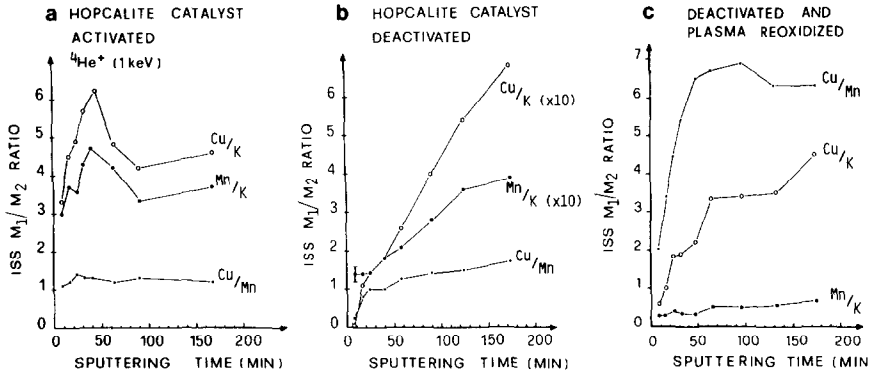

FIG. 8. Depth profiles as obtained from the complete sequence of the ISS spectra shown in Fig. 7. *a*: Activated; *b*: deactivated; *c*: deactivated and plasma reoxidized.

that the adsorption sites for CO and O_2 are blocked. This is in strong contrast with the active catalyst which shows that little potassium is at the surface and Cu and Mn are available for catalysis. Clearly potassium segregation is occurring and covering the active catalyst surface. Plasma reoxidation caused Cu segregation but left the Mn covered by potassium as shown in Fig. 7c.

Depth profiles which summarize the ISS data are given in Fig. 8. The profiles are plotted as ratios of the pertinent components to eliminate any fluctuations of sensitivity during profiling.

To determine if the potassium is equilibrium Gibbsian (*47*) or caused by some other phenomenon, the ISS depth profiles were taken on samples treated at 473, 553, 623, 753, 823, and 873 K along with XPS spectra taken before each ISS experiment. The results are shown in Fig. 9 for both the ISS and XPS intensity ratios. Clearly the potassium segregation does not follow the thermodynamically expected pattern which would decrease monotonically with temperature if kinetically feasible. Segregation occurs at the phase transition as shown by the sharp onset at around 700 K indicated from the ISS curves. The XPS data are in agreement with the ISS results but, as is usual with XPS, its response to changes in the outer surface layer is mitigated by its larger depth sensitivity.

DISCUSSION

The mechanism of deactivation of Hopcalite is in controversy. Schwab and Kanungo (*11*) have reported crystalline $CuMn_2O_4$ to be an active catalyst for CO oxidation. Dondur *et al.* (*7, 8*) and Kanungo (*9, 10*) have reported the activity decreases drastically above the exothermal phase transition. Our results also show that upon the initiation of the phase transition activity begins to decrease. Deactivation is complete at 873 K after 1 to 2 h in nitrogen or oxygen. Kanungo (*9*) attributes the activity of "$CuMn_2O_4$" catalysts to a surface $CuMn_2O_4$ phase. Our results offer a possible explanation of the observations. Pure

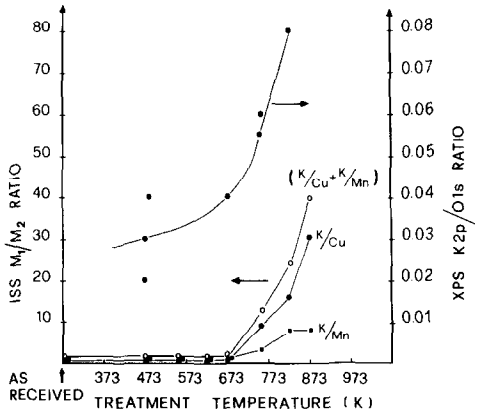

FIG. 9. Segregation of potassium to the surface of Hopcalite catalyst vs temperature.

crystalline $CuMn_2O_4$ may well be active as reported by Schwab and Kanungo (*11*). Hopcalite catalysts containing any impurities or promoters such as alkali metal ions may be subject to phase-change-induced segregation of these species, as found in this work for potassium.

Catalyst Activity and Oxidation States

The importance of oxidation states of Cu and Mn in Hopcalite has recently been emphasized by Schwab and Kanungo (*11*). An "anomalous promotion" was attributed to electron transfer (charge transfer) between Cu and Mn via the redox couple $Mn^{3+} + Cu^{2+} \leftrightharpoons Cu^{1+} + Mn^{4+}$. Although this redox system has been suggested to explain the structural and electronic properties of $CuMn_2O_4$ (*12, 15, 18–20, 23, 24*) and the idea has been indirectly supported by chemical analysis, yields of aldehyde in the oxidation of cinnamyl alcohol and the activity for CO oxidation (*22*), no direct experimental evidence has existed before the present study for this redox system. The evidence from the chemical shifts of the Cu 2*p* line and the multiplet splitting of the Mn 3*s* clearly demonstrates the existence of this redox couple in the Hopcalite catalyst. The redox couple apparently operates in both the amorphous state and the crystalline spinel but is shifted predominantly toward the more stable Cu^{1+}/Mn^{4+} state on crystallization as predicted by Vanderberghe (*24*). Because of the potassium segregation we are not able to tie the redox system directly to catalytic activity. This will have to be explored on ultrapure samples.

The activity of mixed copper oxide and manganese oxide for CO oxidation shows two maxima at ~0.1 and ~0.5 CuO mole fraction (*9, 10, 22*). The minimum in activity occurs in the middle of the composition range. Dollimore and Tonge (*22*) attribute this behavior to the amount of Cu^{1+} in the surface. According to their reasoning, Cu^{1+} forms stable complexes with CO. A high Cu^{1+} surface concentration would give strongly adsorbed CO and block the surface causing lower activity. The highest Cu^{1+} concentration was predicted but not measured to be in the middle of the concentration range. Since in these studies we see Cu^{1+} form at the surface on deactivation, the above explanation would seem to have validity. However, the catalyst in the present study did not reactivate at the oxidizing conditions used for the amorphous samples. Second, plasma-induced reoxidation to Cu^{2+} did not reestablish activity. Thus the potassium segregation which is irreversible and causes catalyst deactivation did not allow us to check the interpretation of Dollimore and Tonge. The true catalytic importance of the oxidation states in the Hopcalite catalyst must be determined in future studies. The clear indication of the redox system as seen in chemical shifts and multiplet splitting indicates this will be possible in future studies. The present results emphasize the need to study the system in a highly pure state free of promoters and dopants.

Segregation

Surface segregation in catalysis is an important phenomenon (*48–50*). Its influence on catalytic activity and selectivity has been demonstrated with Cu–Ni alloys where a small amount of Cu in the bulk produced enormous effects on catalytic behavior (*48–50*). Consequently much work (*47, 51, 52*) has been directed at segregation in alloys. In metals, segregation affects the outer few atomic layers with the dominant change being the outermost monolayer. These studies have been directed at equilibrium segregation where the phenomenon occurs at elevated temperatures sufficient to allow atom mobility. However, it is a decreasing function of temperature in the thermodynamic sense where the higher the temperature the closer the surface composition approaches that of the bulk. The major parameters which control segregation are surface energy, bond energies and atomic size differences. The first parameter

can be influenced by adsorbate bond energy differences and chemically driven segregation can occur under nonvacuum conditions.

Although this is the dominant effect in most systems, lattice strain energy caused by size mismatch controls segregation in some systems and it must always be accounted for.

Segregation in nonmetallic systems has not been sufficiently examined, neither experimentally nor theoretically (*47, 53*). Nevertheless, it can be as important or more important catalytically than in metal systems since catalytic site density related to anion vacancies and inductively induced acidity or basicity can be small on nonmetals. In addition, the effects of segregation can influence several tens of monolayers as compared to 1–5 layers in metals (*54*). The same parameters of surface energy differences and (ionic) size differences will be involved in nonmetals with additional account being taken of electrostatic influences. In the present case the observation of potassium surface enrichment by XPS and ISS mainly involves the latter two.

Potassium segregation occurs at the phase change and causes deactivation of the Hopcalite catalyst. The question arises as to the origin of the segregation. It could be kinetic effect where the temperature of the catalyst must be sufficiently high to allow ion migration. In this case one could expect some exponential dependence on temperature. It could be equilibrium segregation where the extent of segregation is decreased by increasing temperature, barring any kinetic effects, or most likely it is segregation forced by the crystallization of the spinel. The results in Fig. 9 clearly show that it is strictly associated with the phase change. As the amorphous-to-crystalline transition occurs, the ordering of the lattice and the strict ionic size requirements cause the large K^+ ion (ionic radius = 1.33 Å) to move to the surface. In addition, the charge compensation for the Mn^{3+} to Mn^{4+} transition might be partially accounted for by loss of K^+ from the structure. It is known that alkali metal ions stabilize Mn^{3+} in oxide lattices (*55*). The dominant effect, however, is likely to be the large ionic radius of K^+.

During plasma reoxidation of Hopcalite, surface enrichment of copper was observed. Given the strong oxidizing conditions of the plasma it might be expected that the Mn^{4+} would be maintained. However, as the multiplet splitting indicates, both Mn^{4+} and Mn^{3+} are present. The oxidation of Cu^{1+} to Cu^{2+} is still accompanied to some extent by the Mn^{4+} to Mn^{3+} transition. However, Cu^{2+} does segregate to the surface region. In those locations where Mn^{4+} is maintained, conversion of Cu^{1+} to Cu^{2+} causes a charge imbalance and the Cu^{2+} would be expected to migrate to the surface. Thus migration of Cu^{2+} from the charge-imbalanced lattice forming cation-vacancies in the bulk and CuO at the surface may well be the major driving force in an "over-oxidized" system. This is the most direct explanation without becoming involved with the very complex and as yet not firmly established crystallographic properties of the spinel oxide, $CuMn_2O_4$. In this connection, it may be noted that Radhakrishnan and Biswas (*23*) have proposed the following structure:

$$(Cu^{2+}_{0.5}\ Cu^{1+}_{0.25}\ Mn^{3+}_{0.25})_{tet} \cdot [Cu^{2+}_{0.25}\ Mn^{3+}_{1.5}\ Mn^{4+}_{0.25}]_{oct}O^{2-}$$

where the site preference energies have been considered. For a thorough discussion Ref. (*23*) should be consulted.

The proposed surface CuO is suggested by the phase diagram (*56*) and supported by the work of Dollimore and Tonge (*22*) and others (*57*) where CuO was found to be present whenever the oxidation state of manganese was higher than Mn^{3+}. However, no MnO_2 phase was detected by X-ray diffraction indicating Mn^{4+} remains part of the lattice.

Catalyst Activity and Bulk Structure

Schwab and Kanungo (*11*) attributed the

enhanced catalytic activity to the formation of the $CuMn_2O_4$ spinel in Hopcalite catalysts. Others (*7–10*) have seen a loss of activity on the crystallization of the amorphous Hopcalite catalyst. Clearly segregation of K or another component or contaminant driven by the phase change could poison the surface in a manner similar to the findings in this work.

There is growing evidence that the nature of catalytic sites in amorphous systems are not fundamentally different from those found on their crystalline counterparts. However, they differ considerably in concentration at the surface. Larger numbers of sites are being found on amorphous materials than on crystalline materials particularly when these sites involve defect structures (*58*). The smaller number of catalytic sites on crystalline materials has two effects. The catalytic activity decreases on crystallization and the catalyst becomes more susceptible to poisoning.

To correlate Hopcalite catalysis with bulk structure will require well-characterized amorphous and crystalline samples where specific activity is studied (turnover number if possible). These studies must be performed on ultrapure systems since the number of sites on the crystalline materials will be low. Therefore, the correlation between catalytic activity and structure of Hopcalite remains an open question.

CONCLUSION

These studies have produced the following conclusions and questions for future work.

(a) Phase-change-induced segregation can have substantial importance in heterogeneous catalysis. Even impurities and dopants at small levels may appear at the surface and block active sites. This is exacerbated by the decreasing numbers of sites during the amorphous-to-crystalline transition. Potassium segregation is mainly responsible for the deactivation of the Hopcalite catalyst in this study.

(b) The coupled redox system

$$Cu^{2+} + Mn^{3+} \rightleftharpoons Cu^{1+} + Mn^{4+}$$

has been experimentally confirmed using XPS chemical shift and shake-up information on Cu, and multiplet splitting on Mn. This interesting and important phenomenon is now open for further investigation.

(c) The activity–structure correlations on Hopcalite catalysts must be done on highly pure materials, thus avoiding the phenomenon of phase-change-induced segregation. The turnover number also must be established to investigate the quality of the catalytic sites on the amorphous and crystalline systems.

(d) The importance of a multiple technique approach to catalyst characterization involving both primary structural probes as well as surface analysis has been demonstrated.

This paper lays the groundwork for future detailed investigations of amorphous and crystalline oxide systems, in particular mixed Cu- and Mn-oxide catalysts.

ACKNOWLEDGMENTS

The authors thank Dr. A. Wyttenbach for performing the neutron activation analysis of the samples used in this work. A partial financial support by the Swiss National Research Foundation is acknowledged.

REFERENCES

1. Jones, H. A., and Taylor, H. S., *J. Phys. Chem.* **27,** 623 (1923).
2. Lamb, A. B., Bray, W. C., and Frazer, J. C. W., *Ind. Eng. Chem.* **12,** 213 (1920).
3. Stone, F. S., "Advances in Catalysis," Vol. 13, p. 1. Academic Press, New York, 1962.
4. Jagow, R. B., Katan, T., Lamparter, R. A., and Ray, C. D., American Society of Mechanical Engineers, ASME Technical Report 77-ENAS-28.
5. Margolis, L. Y., *Catal. Rev. Sci. Eng.* **8,** 241 (1973).
6. Klauer, F., "Significant Information of Respiratory Protection," paper presented at 1967 Mine Rescue Superintendents Conference (National Coal Board), published by the Auergesellschaft GMBH, Berlin, 1967.
7. Dondur, V., Lampa, S., and Vucelic, D., *in* "Proc., Second European Symposium on Thermal Analysis" (D. Dollimore, Ed.). Heden, London (1981).
8. Dondur, V., Lampa, S., and Vucelic, D., *in* "Het-

erogeneous Catalysis," Proc., 4th Int. Symposium, Part 2, 1979, p. 151 and Proc., 2nd Europ. Symp. Thermal Anal. (D. Dollimore Ed.), p. 182. Heyden, London, 1981.
9. Kanungo, S. B., "Symposium on Science of Catalysis and Its Application in Industry FPDIL, Sindri, India, 1979."
10. Kanungo, S. B., *J. Catal.* **58,** 419 (1979).
11. Schwab, G. M., and Kanungo, S. B., *Z. Phys. Chem. N.F.* **107,** 109 (1977).
12. Sinha, A. P. B., Sanjana, N. R., and Biswas, A. B., *J. Phys. Chem.* **62,** 191 (1958).
13. Zaslavskii, A. I., Karachentseva, Z. V., and Zharinova, A. I., *Kristallografiya* **7,** 835 (1962).
14. Miyahara, S., *J. Phys. Soc. Japan* **17** B-1, 181 (1962).
15. Blasse, G., *J. Phys. Chem. Solids* **27,** 383 (1966).
16. Lopatin, E., and Baltzer, P. K., *Phys. Rev. Lett.* **22,** 380 (1966).
17. Miller, A., *J. Phys. Chem. Solids* **29,** 633 (1968).
18. Sabane, C. D., Sinha, A. P. B., and Biswas, A. B., *Indian J. Pure Appl. Phys.* **4,** 187 (1966).
19. Jogalekar, P. P., and Sinha, A. P. B., *Indian J. Pure Appl. Phys.* **5,** 9 (1967).
20. Naik, B. N., and Sinha, A. P. B., *Indian J. Pure Appl. Phys.* **2,** 170 (1969).
21. Padalia, B. D., Krishnan, V., Patni, M. J., Radhakrishnan, N. K., and Gupta, S. N., *J. Phys. Chem. Solids* **34,** 1173 (1973).
22. Dollimore, D., and Tonge, K. H., *J. Chem. Soc. A,* 1728 (1970).
23. Radhakrishnan, N. K., and Biswas, A. B., *Phys. Status Solidi* **44,** 45 (1977).
24. Vanderberghe, R. E., *Phys. Status Solidi* **50,** K85 (1978).
25. Knözinger, H., "Advances in Catalysis," Vol. 25, p. 184. Academic Press, New York, 1976.
26. Knözinger, H., *Catal. Rev. Sci. Eng.* **17,** 31 (1978).
27. Wahl, K., and Klemm, W., *Z. Anorg. Allg. Chem.* **270,** 69 (1952).
28. Happel, J., Kiang, S., Spencer, J. L., Oki, S., and Hnatow, M. Z., *J. Catal.* **50,** 429 (1977).
29. Kobayashi, M., Matsumoto, H., and Kobayashi, H., *J. Catal.* **21,** 48 (1971).
30. Schwab, G. M., and Block, J., *Z. Phys. Chem. N.F.* **1,** 42 (1954).
31. Dadyburjor, D. B., Jewar, S. S., and Ruckenstein, E., *Catal. Rev. Sci. Eng.* **19,** 293 (1979).
32. Jap. Pat. Hopcalite Catalyst, Pat. No. 76-20477, 1976.
33. Kehl, S., Diploma thesis, University of Zurich, August, 1983.
34. Vepřek, S., *Pure Appl. Chem.* **48,** 163 (1976); **54,** 119 (1982).
35. Delannay, F., and Delmon, B., *in* "Characterization of Heterogeneous Catalysts" (F. Delannay, Ed.), Vol. 1. Dekker, New York, 1984.
36. Putanov, P., Neducin, R. M., Lomic, G., Genova, M., and Kis, E., *in* "Proceedings, 8th International Congress on Catalysis, Berlin, 1984," Vol. V, p. 335. Verlag Chemie, Basel, 1984.
37. Buhl, R., *J. Phys. Chem. Solids* **30,** 805 (1969).
38. Dreiling, M. J., *J. Phys. Chem. Solids* **37,** 121 (1976).
39. Frost, D. C., Ishitani, A., and McDowell, C. A., *Mol. Phys.* **24,** 861 (1972).
40. D'Huysser, A., Lerebours-Hannoyer, B., Lenglet, M., and Bonnelle, J. P., *J. Solid State Chem.* **39,** 246 (1981).
41. D'Huysser, A., Luchetti, A., Wrobel, G., and Bonnelle, J. P., *J. Microsc. Spectrosc. Electron* **2,** 609 (1977).
42. Haber, J., Machej, T., Ungier, L., and Ziółkowski, J., *J. Solid State Chem.* **25,** 207 (1978).
43. Brabers, V. A. M., van Setten, F. M., and Knapen, P. S. A., *J. Solid State Chem.* **49,** 93 (1983).
44. Shirley, D. A., *Phys. Scr.* **11,** 117 (1975).
45. Horrell, B., and Cocke, D. L., submitted for publication.
46. Horrell, B., Cocke, D. L., Sparrow, G., and Murray, J., *J. Catal.*, in press.
47. Somorjai, G. "Chemistry in Two Dimensions: Surfaces." Cornell Univ. Press, Ithaca, 1981.
48. van der Plank, P., and Sachtler, W. M. H., *J. Catal.* **12,** 35 (1968).
49. Sinfelt, J. H., Carter, J. L., and Yates, D. J. C., *J. Catal.* **24,** 283 (1972).
50. Ponec, V., and Sachtler, W. M. H., *J. Catal.* **24,** 250 (1972).
51. Johnson, W. C., and Blakely, J. M., Eds., "Interfacial/Segregation." Amer. Soc. Met., New York, 1979.
52. Overbury, S. H., Betrand, P. A., and Somorjai, G. A., *Chem. Rev.* **75,** 547 (1975).
53. Nowotny, J., Sikora, I., and Wagner, Jr., J. B., *Mater. Sci. Monogr.* **15,** 244 (1982).
54. Haber, J., *in* "Surface Properties and Catalysis by Non-Metals" (J. P. Bonnelle, B. Delmon, and E. Derouane, Eds.). p. 1. Reidel, Boston, 1982.
55. Cimino, A., Lo Jacono, M., Porta, P., and Valigi, M., *Z. Phys. Chem. N.F.* **59,** 134 (1968).
56. Tretyakov, Y. D., Komarov, V. F., Prosvirnina, N. A., and Kutsenok, I. B., *J. Solid State Chem.* **5,** 157 (1972).
57. Kurlina, E. V., Prokhvatilov, V. G., and Sheftes, I. T., *Dokl. Akad. Nauk SSSR* **86,** 305 (1952).
58. Yoon, C.-H., and Cocke, D. L., *J. Non-Cryst. Solids,* in press.